

# Direct In Situ Investigation of Milling Reactions Using Combined X-ray Diffraction and Raman Spectroscopy\*\*

Lisa Batzdorf, Franziska Fischer, Manuel Wilke, Klaus-Jürgen Wenzel, and Franziska Emmerling\*

**Abstract:** The combination of two analytical methods including time-resolved in situ X-ray diffraction (XRD) and Raman spectroscopy provides a new opportunity for a detailed analysis of the key mechanisms of milling reactions. To prove the general applicability of our setup, we investigated the mechanochemical synthesis of four archetypical model compounds, ranging from 3D frameworks through layered structures to organic molecular compounds. The reaction mechanism for each model compound could be elucidated. The results clearly show the unique advantage of the combination of XRD and Raman spectroscopy because of the different information content and dynamic range of both individual methods. The specific combination allows to study milling processes comprehensively on the level of the molecular and crystalline structures and thus obtaining reliable data for mechanistic studies.

Over the past decade, mechanochemistry has attracted significant interest as a fast and effective method for obtaining pure compounds.<sup>[1]</sup> The method is a promising alternative synthesis strategy for inorganic, metal-organic, and organic compounds.<sup>[1a,2]</sup> Despite the wide application of mechanochemistry the mechanisms of milling reactions are not fully understood. Typically, mechanistic information is derived from ex situ experiments which include an interruption of the synthesis for sample drawing.<sup>[3]</sup> Air-sensitive or fast converting intermediates and fast phase changes cannot be detected under these conditions. In addition, products resulting from an interrupted synthesis might differ from those obtained in a continuous synthesis.<sup>[1b,4]</sup> So far, the inability to monitor these reactions directly in situ precludes detailed mechanistic studies.

Pioneering in situ investigations of milling processes using either Raman spectroscopy or synchrotron X-ray diffraction have been reported recently.<sup>[5]</sup> To access complete and comprehensive information on the reaction mechanisms, there is a necessity to combine XRD and Raman spectroscopy in one experiment. This combination has the following

immediate advantages: 1) an integral information on the composition of the crystalline material, its transitions, and crystallite size together with 2) information on the molecular level of either crystalline, nanocrystalline, amorphous, liquid, or volatile phases. When studying milling reactions under realistic conditions, it is even more appropriate to rely on two methods in order to exclude measurement artifacts. Consequently, the combination of these methods in one experiment presented here allows to observe simultaneously the complete formation process on the molecular and crystalline level. The formation of the MOFs ZIF-8 (**1**) and (H<sub>2</sub>Im)[Bi(1,4-bdc)<sub>2</sub>] (**2**), the metal phosphonate CoPhPO<sub>3</sub>·H<sub>2</sub>O (**3**), and the 1:1 cocrystal theophylline:benzoic acid (TP:BA) (**4**) were analyzed under realistic milling conditions to examine the applicability of the setup.

Figure 1 a shows the setup including the ball mill, a Perspex grinding jar, the Raman probe head, and the optical path with CCD detector for XRD. The experiments were performed at frequencies between 30 to 50 Hz covering reaction times of 15 or 30 minutes. Raman spectra and XRD patterns

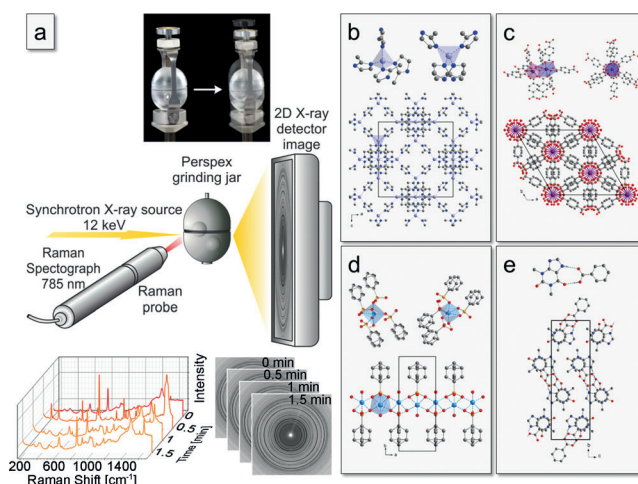


**Figure 1.** a) Schematic diagram of the experimental setup for collecting Raman spectra and XRD powder patterns during the mechanochemical synthesis. Raman spectra and XRD patterns were typically collected every 30 s. The vibration ball mill is used with 10 mL Perspex grinding jars and two 10 mm stainless steel grinding balls. During the measurements the grinding jar oscillates around the position of measurement. b–e) View of the crystal structures of the investigated metal-organic frameworks ZIF-8 (Zn(Melm)<sub>2</sub> (Melm = 2-methylimidazolate)) **1** and (H<sub>2</sub>Im)[Bi(1,4-bdc)<sub>2</sub>] (Im = imidazole, bdc = benzenedicarboxylate) **2**, the metal phosphonate cobalt(II) phenylphosphonate monohydrate CoPhPO<sub>3</sub>·H<sub>2</sub>O (Ph = phenyl) **3**, and the cocrystal theophylline:benzoic acid (1:1) **4**.

[\*] M. Sc. L. Batzdorf,<sup>[‡]</sup> Dipl.-Chem. F. Fischer,<sup>[‡]</sup> Dipl.-Chem. M. Wilke,<sup>[‡]</sup> Dipl.-Ing. K.-J. Wenzel, Dr. F. Emmerling  
BAM Federal Institute for Materials Research and Testing  
Richard-Willstätter-Str. 11, 12489 Berlin (Germany)  
E-mail: franziska.emmerling@bam.de

[‡] These authors contributed equally to this work.

[\*\*] We gratefully acknowledge financial support by the DFG through SPP 1415 (grant number Em198/5-2).

Supporting information for this article is available on the WWW under <http://dx.doi.org/10.1002/anie.201409834>.

were collected every 30 seconds. The experiments can be carried out under characteristic and realistic synthesis conditions in typical quantities and volumes. These experiments represent, to the best of our knowledge, the first study of this kind. The results promise a wide applicability of this approach for mechanistic studies of milling reactions.

The mechanochemical synthesis of the metal–organic framework ZIF-8 **1** was investigated under ionic-liquid-assisted grinding (ILAG) conditions (Figure 1b). Zinc oxide and 2-methylimidazole were ground together in the presence of small amounts of ammonium nitrate and dimethylformamide (DMF). The in situ diffraction patterns and simultaneously recorded Raman spectra are shown in Figure S2 (see the Supporting Information) together with a detailed description. The data obtained reveal a direct reaction to the final product which proceeds within 2 minutes milling time. The Raman spectra indicate a decelerated adjustment of the 2-methylimidazolate molecule in the crystal structure of **1**.

The compound  $(\text{H}_2\text{Im})[\text{Bi}(1,4\text{-bdc})_2]$  **2** (Figure 1c) was chosen since ex situ investigation using standard laboratory XRD measurements and Raman spectroscopy indicated the existence of an intermediate phase.<sup>[3 h, 6]</sup> Figure 2 shows the in situ data acquired during the mechanochemical synthesis of **2**. The synthesis is performed by milling bismuth(III) nitrate pentahydrate and terephthalic acid together with an excess of imidazole for 15 minutes. The combination of XRD and Raman spectroscopy reveals the fast formation of the intermediate starting from bismuth(III) nitrate pentahydrate and imidazole within 1 minute. Both sets of data indicate that the product is synthesized quickly from the intermediate and terephthalic acid. Additionally, both methods indicate a milling period until 6.5 minutes where the product **2** and terephthalic acid are present in the reaction mixture before the pure product is gained as white powder.

The XRD patterns reveal a completed conversion of the starting materials (Figure 2a, yellow) bismuth(III) nitrate pentahydrate and imidazole after a milling time of 1 minute, whereas terephthalic acid is still present in the XRD pattern of the reaction mixture. Bismuth(III) nitrate pentahydrate and imidazole form an intermediate which is characterized by a strong reflection at  $6.5^\circ$  (Figure 2a, blue). The powder pattern is in good agreement with the diffractogram of the basic bismuth nitrate  $\text{Bi}_6\text{O}_5(\text{OH})_3(\text{NO}_3)_5(\text{H}_2\text{O})_3$ .<sup>[7]</sup> After a milling period of 2.5 minutes the XRD pattern indicates the reaction of the intermediate with the unchanged terephthalic acid to form **2**. The reflections of the intermediate vanish directly whereas pure terephthalic acid can be detected for a prolonged milling time of 6 minutes (Figure 4a, purple). The product is formed and remains stable during prolonged milling time (Figure 2a, red). These findings are backed by the simultaneously collected Raman spectra (see detailed description in the Supporting Information section). Furthermore, the protonation of imidazole

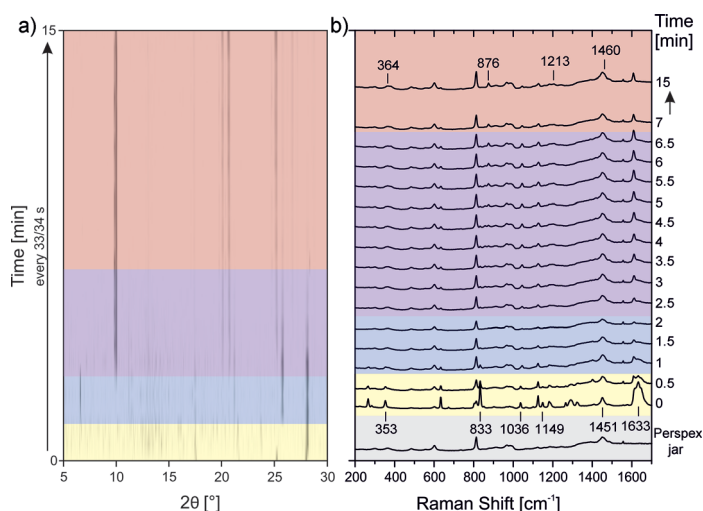


**Figure 2.** Synthesis process of the metal–organic framework  $(\text{H}_2\text{Im})[\text{Bi}(1,4\text{-bdc})_2]$  **2** followed in situ by a) synchrotron XRD and b) Raman spectroscopy. The first measurement of the Raman plot (gray) is the Raman spectrum of the empty Perspex jar, indicating which modes of the following synthesis process arise from the sample holder and which from the reaction mixture. Yellow: reactants, blue: intermediate (activated  $\text{Bi}^{3+}$  species) and terephthalic acid, purple: product **2** and terephthalic acid, red: product.

during the formation of the intermediate is confirmed by the Raman data.

The mechanochemical synthesis of the metal phosphonate cobalt(II) phenylphosphonate monohydrate ( $\text{CoPhPO}_3 \cdot \text{H}_2\text{O}$ , **3** Figure 1d) was chosen as a model compound for layered structures. The reactants cobalt(II) acetate tetrahydrate and phenylphosphonic acid were ground together in an equimolar ratio. The data obtained in situ is consistent with a two-step formation process comprising an intermediate (Figure 3).

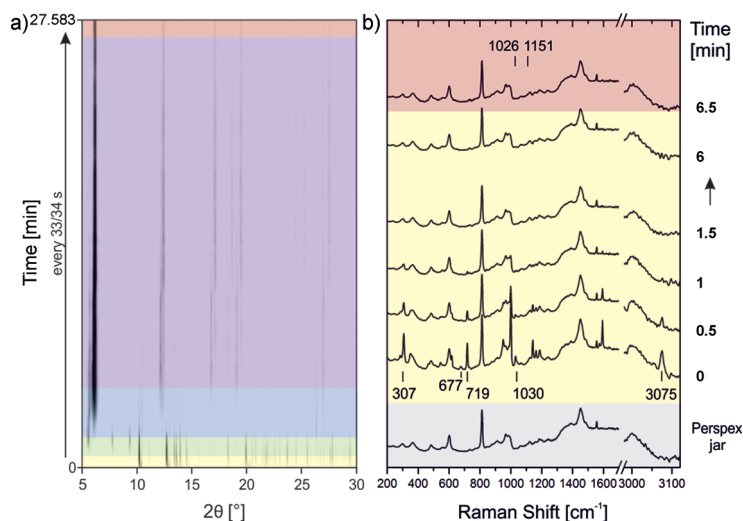


**Figure 3.** Synthesis process of  $\text{CoPhPO}_3 \cdot \text{H}_2\text{O}$  **3** followed in situ by a) synchrotron XRD and b) Raman spectroscopy. The first measurement of the Raman plot (gray) is the Raman spectrum of the empty Perspex jar, indicating which modes of the following synthesis process arise from the sample holder compared to those from the reaction mixture. Yellow: Reactants, green: reactants and intermediate phases, blue: reactants, intermediate phases and product, purple: intermediate phases and product, red: product.

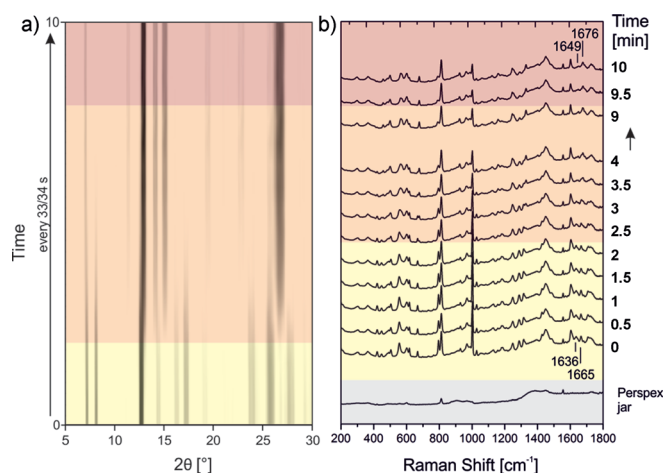


**Figure 4.** Synthesis process of the cocrystal TP:BA **4** followed in situ by a) synchrotron XRD and b) Raman spectroscopy. The first measurement of the Raman plot (gray) is the Raman spectrum of the empty Perspex jar, indicating which modes of the following synthesis process arise from the sample holder and which from the reaction mixture. Yellow: reactants, orange: reactants and product, red: product.

After an initial phase where only the reactants can be detected (Figure 3a, yellow), the XRD patterns indicate the formation of a layered intermediate structure which is formed after 1 minute milling time (Figure 3a, green). Since contributions of phenylphosphonic acid cannot be detected in the XRD patterns but in the Raman data after the appearance of this intermediate, it can be supposed that the acid is arranged between the layers acting as a template. The first reflection of the product **3** could be detected after 2.75 minutes (Figure 5a, blue).<sup>[8]</sup> Intermediate and product coexist for a certain period of time (Figure 3a, violet) until the conversion to **3** is completed after a milling time of 27 minutes (Figure 5a, red).

The synthesis of the cocrystal TP:BA **4** (Figure 1e) was conducted under neat conditions starting from pure theophylline and benzoic acid. Based on the time-resolved diffraction

patterns and the Raman spectra (Figure 4) a direct reaction without formation of any intermediates can be deduced.

At the beginning of the milling process only reflections of the reactants can be observed in the powder pattern (Figure 4a, yellow). The first reflections of the product appear after 2 minutes milling time (Figure 4a, orange), whereas the reflections of the reactants are still observable. With prolonged milling time the reflections of the product increase and those of the reactants diminish. After a milling time of 8 minutes the pure cocrystal is formed (Figure 4a, red). In accordance to the XRD data the first Raman spectra can be attributed to the reactants theophylline and benzoic acid. The first Raman bands assigned to the product appear after 1.5 minutes (Figure 4b, orange). The Raman spectrum of the cocrystal **4** resembles the spectrum of the starting materials. Given the fact that cocrystals generally only involve the formation of hydrogen bonds that are different from those associated with the individual components themselves, only minor changes in the spectra are expected. The Raman modes of theophylline at 1665 and 1707  $\text{cm}^{-1}$  (carbonyl bands) were analyzed in detail to decide if there is a complete shift of the acid proton between theophylline and benzoic acid. By forming a salt, these carbonyl bands would shift by 30–40  $\text{cm}^{-1}$  to lower frequencies.<sup>[9]</sup> The carbonyl bands of the theophylline molecule in the cocrystal shifted to 1676 and 1687  $\text{cm}^{-1}$  because of the formation of new hydrogen bonds. Since the carbonyl band of benzoic acid at 1636  $\text{cm}^{-1}$  shifting by 13  $\text{cm}^{-1}$  is also not strongly influenced in the cocrystal, it can be assumed that the cocrystal consists of neutral molecules and no salt is formed.

The presented in situ combination of Raman spectroscopy and XRD is capable to monitor the course of mechanochemical reactions in detail at the molecular and crystalline level. The setup allows performing and analyzing milling reactions under typical reaction conditions. The information content obtained by one method is supported or extended by the second method (e.g. detection of nanocrystalline material using Raman spectroscopy versus unambiguous assignment of the polymorph using XRD), making the combination of both methods a reliable tool to study milling reactions in situ. For the four model compounds comprehensive information on the respective synthesis pathways could be obtained as illustrated in Figure 5. The synthesis of compounds **1** and **4** proceed directly through the consumption of the reactants (A). During the synthesis of compounds **2** and **3** crystalline intermediates were detected (B).

Beyond the presented results, the combination of both methods would also be advantageous studying milling reactions including amorphous intermediates. Here, Raman spectroscopy would provide important information on the local coordination environment. Our results show that the setup is applicable for a broad range of compounds and milling conditions. This measurement strategy will broaden our understanding of the mechanisms of milling syntheses and thus allows an optimization of the reactions.

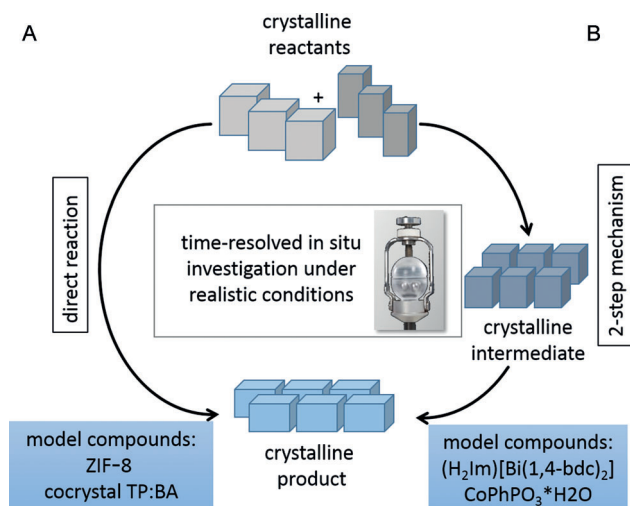


**Figure 5.** Schematic representation of the two observed synthesis pathways (A and B) indicating an either A) direct conversion or B) a two-step process including a crystalline intermediate.

Received: October 7, 2014  
Published online: December 21, 2014

**Keywords:** mechanochemistry · milling reactions · reaction mechanisms · Raman spectroscopy · X-ray diffraction

- [1] a) S. L. James, C. J. Adams, C. Bolm, D. Braga, P. Collier, T. Frisčić, F. Grepioni, K. D. M. Harris, G. Hyett, W. Jones, A. Krebs, J. Mack, L. Maini, A. G. Orpen, I. P. Parkin, W. C. Shearouse, J. W. Steed, D. C. Waddell, *Chem. Soc. Rev.* **2012**, *41*, 413–447; b) A. A. L. Michalchuk, I. A. Tumanov, E. V. Boldyreva, *CrystEngComm* **2013**, *15*, 6403–6412; c) A. Stolle, T. Szuppa, S. E. S. Leonhardt, B. Ondruschka, *Chem. Soc. Rev.* **2011**, *40*, 2317–2329.
- [2] a) T. Frisčić, D. G. Reid, I. Halasz, R. S. Stein, R. E. Dinnebier, M. J. Duer, *Angew. Chem. Int. Ed.* **2010**, *49*, 712–715; *Angew. Chem.* **2010**, *122*, 724–727; b) D. Braga, L. Maini, F. Grepioni, *Chem. Soc. Rev.* **2013**, *42*, 7638–7648; c) D. Braga, F. Grepioni, *Angew. Chem. Int. Ed.* **2004**, *43*, 4002–4011; *Angew. Chem.* **2004**, *116*, 4092–4102; d) L. Tröbs, A. Zimathies, U. Panne, F. Emmerling, *Z. Phys. Chem.* **2014**, *228*, 575–585; e) M. Klimakow, P. Klobes, K. Rademann, F. Emmerling, *Microporous Mesoporous Mater.* **2012**, *154*, 113–118; f) F. Fischer, G. Scholz, S. Benemann, K. Rademann, F. Emmerling, *CrystEngComm* **2014**, *16*, 8272–8278; g) M. Klimakow, P. Klobes, A. F. Thunemann, K. Rademann, F. Emmerling, *Chem. Mater.* **2010**, *22*, 5216–5221; h) G. A. Bowmaker, *Chem. Commun.* **2013**, *49*, 334–348; i) N. Shan, F. Toda, W. Jones, *Chem. Commun.* **2002**, 2372–2373.
- [3] a) X. H. Ma, W. B. Yuan, S. E. J. Bell, S. L. James, *Chem. Commun.* **2014**, *50*, 1585–1587; b) M. R. Caira, L. R. Nassimbeni, A. F. Wildervanck, *J. Chem. Soc. Perkin Trans. 2* **1995**, 2213–2216; c) K. D. M. Harris, *Nat. Chem.* **2013**, *5*, 12–14; d) T. Rojac, B. Malic, M. Kosec, M. Polomska, B. Hilczer, B. Zupancic, B. Zalar, *Solid State Ionics* **2012**, *215*, 1–6; e) G. Kozma, A. Kukovecz, Z. Konya, *J. Mol. Struct.* **2007**, *834*, 430–434; f) I. A. Tumanov, A. F. Achkasov, E. V. Boldyreva, V. V. Boldyrev, *CrystEngComm* **2011**, *13*, 2213–2216; g) F. Fischer, G. Scholz, S. Benemann, K. Rademann, F. Emmerling, *CrystEngComm* **2014**, *16*, 8272–8278.
- [4] a) V. Strukil, L. Fábián, D. G. Reid, M. J. Duer, G. J. Jackson, M. Eckert-Maksic, T. Frisčić, *Chem. Commun.* **2010**, *46*, 9191–9193; b) V. V. Boldyrev, *Usp. Khim.* **2006**, *75*, 203–216.
- [5] a) I. Halasz, A. Puskaric, S. A. J. Kimber, P. J. Beldon, A. M. Belenguer, F. Adams, V. Honkimaki, R. E. Dinnebier, B. Patel, W. Jones, V. Strukil, T. Frisčić, *Angew. Chem. Int. Ed.* **2013**, *52*, 11538–11541; *Angew. Chem.* **2013**, *125*, 11752–11755; b) I. Halasz, S. A. J. Kimber, P. J. Beldon, A. M. Belenguer, F. Adams, V. Honkimaki, R. C. Nightingale, R. E. Dinnebier, T. Frisčić, *Nat. Protoc.* **2013**, *8*, 1718–1729; c) D. Gracin, V. Strukil, T. Frisčić, I. Halasz, K. Uzarevic, *Angew. Chem. Int. Ed.* **2014**, *53*, 6193–6197; *Angew. Chem.* **2014**, *126*, 6307–6311; d) H. L. Lin, G. C. Zhang, P. C. Hsu, S. Y. Lin, *Microchem. J.* **2013**, *110*, 15–20.
- [6] L. Tröbs, M. Wilke, W. Szczerba, U. Reinholz, F. Emmerling, *CrystEngComm* **2014**, *16*, 5560–5565.
- [7] a) F. Lazarini, *Acta Crystallogr. Sect. B* **1978**, *34*, 3169–3173; b) B. Liu, W. W. Zhou, Z. Q. Zhou, X. Y. Zhang, *Inorg. Chem. Commun.* **2007**, *10*, 1145–1148.
- [8] T. O. Salami, X. Fan, P. Y. Zavalij, S. R. J. Oliver, *Dalton Trans.* **2006**, 1574–1578.
- [9] a) J. Madarász, P. Bombicz, K. Jármi, M. Bán, G. Pokol, S. Gál, *J. Therm. Anal.* **2002**, *69*, 281–290; b) J. Lu, S. Rohani, *Org. Process Res. Dev.* **2009**, *13*, 1269–1275.